PNAS
www.pnas.org

Supplementary Information for

Seasonal changes in NRF2 antioxidant pathway regulates winter depression-like behavior

Tomoya Nakayama[1-3‡], Kousuke Okimura[1,2‡], Jiachen Shen[1,2‡], Ying-Jey Guh[1,3‡], T. Katherine Tamai[1], Akiko Shimada[1,2], Souta Minou[1,2], Yuki Okushi[1,2], Tsuyoshi Shimmura[2,3]†, Yuko Furukawa[1], Naoya Kadofusa[1], Ayato Sato[1], Toshiya Nishimura[4], Minoru Tanaka[4], Kei Nakayama[5,6], Nobuyuki Shiina[5,6], Naoyuki Yamamoto[7], Andrew S. Loudon[8], Taeko Nishiwaki-Ohkawa[1,2], Ai Shinomiya[3,6,9], Toshitaka Nabeshima[10], Yusuke Nakane[1,2], and Takashi Yoshimura[1-3*]

[1]Institute of Transformative Bio-Molecules (WPI-ITbM), Nagoya University, Nagoya 464-8601, Japan. [2]Laboratory of Animal Integrative Physiology, Graduate School of Bioagricultural Sciences, Nagoya University, Nagoya 464-8601, Japan. [3]Division of Seasonal Biology, National Institute for Basic Biology, National Institutes of Natural Sciences, Okazaki, Aichi 444-8585, Japan. [4]Graduate School of Science, Nagoya University, Nagoya 464-8601, Japan. [5]Laboratory of Neuronal Cell Biology, National Institute for Basic Biology, National Institutes of Natural Sciences, Okazaki 444-8585, Japan. [6]Department of Basic Biology, The Graduate University for Advanced Studies (SOKENDAI), Miura, Kanagawa 240-0193, Japan. [7]Laboratory of Fish Biology, Graduate School of Bioagricultural Sciences, Nagoya University, Nagoya 464-8601, Japan. [8]Centre for Biological Timing, Faculty of Biology, Medicine and Health, School of Medical Sciences, The University of Manchester, Oxford Rd, Manchester M13 9PL, UK. [9]Exploratory Research Center on Life and Living Systems, National Institutes of Natural Sciences, Okazaki, Aichi 444-8787, Japan. [10]Advanced Diagnostic System Research Laboratory, Fujita Health University Graduate School of Health Science, Toyoake, Aichi 470-1192, Japan. †Present address: Department of Biological Production, Tokyo University of Agriculture and Technology, Fuchu, Tokyo 183-8509, Japan.

*Address correspondence to:
Takashi Yoshimura, Ph.D., FRSB
Email: takashiy@agr.nagoya-u.ac.jp

This PDF file includes:

Supplementary text
Figures S1 to S9
Legends for Tables S1 to S7
SI References

Other supplementary materials for this manuscript include the following:

Tables S1 to S7

www.pnas.org/cgi/doi/10.1073/pnas.2000278117

SI Materials and Methods

Analysis of spine density. DiI (1 mg, Thermo Fisher Scientific) was dissolved into 100 µl of methylene chloride and then spread onto a glass slide with aliquots of 100 mg tungsten bead (suspended in 100 µl methylene chloride). After the methylene chloride evaporated completely, beads were scraped off the glass slide and cut into a fine powder. All the DiI-coated tungsten particles were then suspended into 1 ml of water, and sonicated in a water bath for 30-60 min at room temperature. The delivery of DiI-coated tungsten particles into the fixed brain slice (200 µm of thickness) was conducted by the biolistic bombardment using Bio-Rad Biolistic PDS-1000/He particle delivery system following the manufacture's instruction. 10 µl of DiI-coated tungsten particle suspension was loaded on to the microcarrier (Bio-Rad), and the bombardment was performed with 1100 psi Helium pressure under a 9 cm of target distance. After bombardment, the brain slices were washed 3 times with phosphate buffered salts (PBS), and then stored in PBS for 2-5 hours in the dark at room temperature to allow the DiI to diffuse through the neurons. Slices then were mounted onto a glass slide with ProLong Gold Antifade (Thermo Fisher Scientific) and covered with an 18 × 18 mm coverslip. Z-stack fluorescence images were acquired using the Nikon A1 confocal microscope with a 63 × oil objective lens and the density and morphology of dendritic spines were analyzed by NeuronStudio, a software designed for detection of 3D spine morphology (1). The voxel size of the image was 0.07 × 0.07 × 0.125 µm, and the spines were automatically detected and classified as"mushroom," "thin," or "stubby" by the software using the criteria (default) as follows: Neck ratio: spines with head to neck diameter ratio greater than 1.1 are considered thin or mushroom; Thin ratio: spines that do not meet the neck ratio value and have a length to spine to head diameter above 2.5 are classified as thin, otherwise as stubby; Mushroom size: spines that meet the neck ratio value 1.1 and have a head diameter equal or greater than 0.35 µm are labeled as mushroom, otherwise as stubby. Some protrusions missed by the algorithm were added and classified manually and the false labeling of other structures as spines were deleted. For each condition, dendritic segment images were acquired from 5 male fish (6-8 segments per fish) and all the images have been analyzed by two researchers independently.

***In situ* hybridization (ISH).** Expression of *OPN4B* and *NRF2* was analyzed using DIG-labeled RNA probes. As previously described (2), the head of medaka in SC and LW conditions were fixed in 4 % paraformaldehyde in phosphate-buffered saline (pH 7.4), and paraffin-embedded sections were cut at a thickness of 8 µm. The probes for *OPN4B* and *NRF2* were amplified with gene-specific primers (*OPN4B*: Forward: 5' - cacaaccccatcatttatgc - 3'; Reverse: 5' - ctgtccagttgttcatggta - 3'; *NRF2*: Forward: 5' - tttcgactacaaccatcggca - 3'; Reverse: 5' - taggagccccctccataagc - 3') and cloned into pCR-II-TOPO (Invitrogen), followed by linearization and *in vitro* transcription (Roche Life Science). Tissue sections were treated with proteinase K (3 µg/mL) and subsequently hybridized with DIG-labeled RNA probes. Hybridization signals were detected using an alkaline phosphatase-conjugated anti-DIG antibody (Roche Life Science), with Nitro Blue tetrazolium and 5-bromo-4-chloro-3-indolyl-phosphate as the chromogen.

Expression of *OPN4XB* was analyzed using RNAscope (Advanced Cell Diagnostics) following the manufacturer's guidelines. The heads of SC and LW fish were fixed in 4% paraformaldehyde in phosphate-buffered saline (pH 7.4), and paraffin-embedded sections were cut at a thickness of 8 µm. Slides were processed as described in the RNAscope protocol using the RNAscope 2.5 HD Reagent Kit and probe for *OPN4XB*.

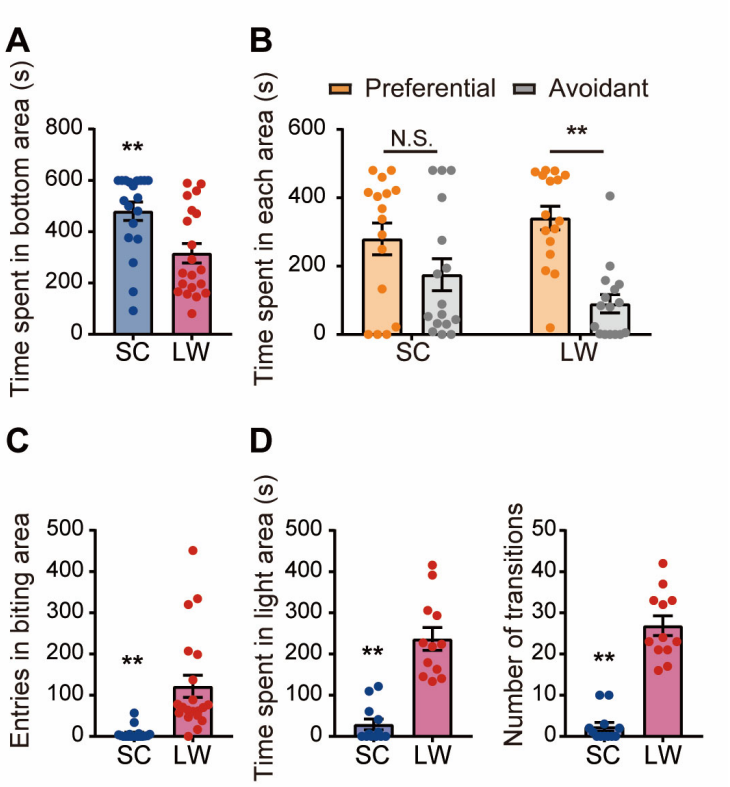

Fig. S1. Similar to males, female medaka are also less social and show more anxiety-like behaviors under winter-like conditions. (*A*) Female medaka spent less time at the bottom of the tank in long-day and warm-temperature (LW) conditions than when kept under short-day and cool-temperature (SC) conditions (Welch's *t*-test, $^{**}P < 0.01$, mean ± SEM, n = 19-20). (*B*) Female medaka kept under LW conditions spent more time in the preferential area, whereas those kept under SC conditions failed to show any interest in other fish (two-way ANOVA and Sidak's multiple comparison test. $^{**}P < 0.01$, N.S. is not significant, mean ± SEM, n = 16). (*C*) The number of crossings into the mirror contact zone was significantly decreased under SC compared with LW conditions. (Welch's *t*-test, $^{**}P < 0.01$, mean ± SEM, n = 18-20). (*D*) Female medaka in LW conditions spent more time in the light area than when kept in SC conditions. Also, female medaka kept under LW conditions showed significantly more transitions between light and dark areas. (Welch's *t*-test, $^{**}P < 0.01$, mean ± SEM, n = 12).

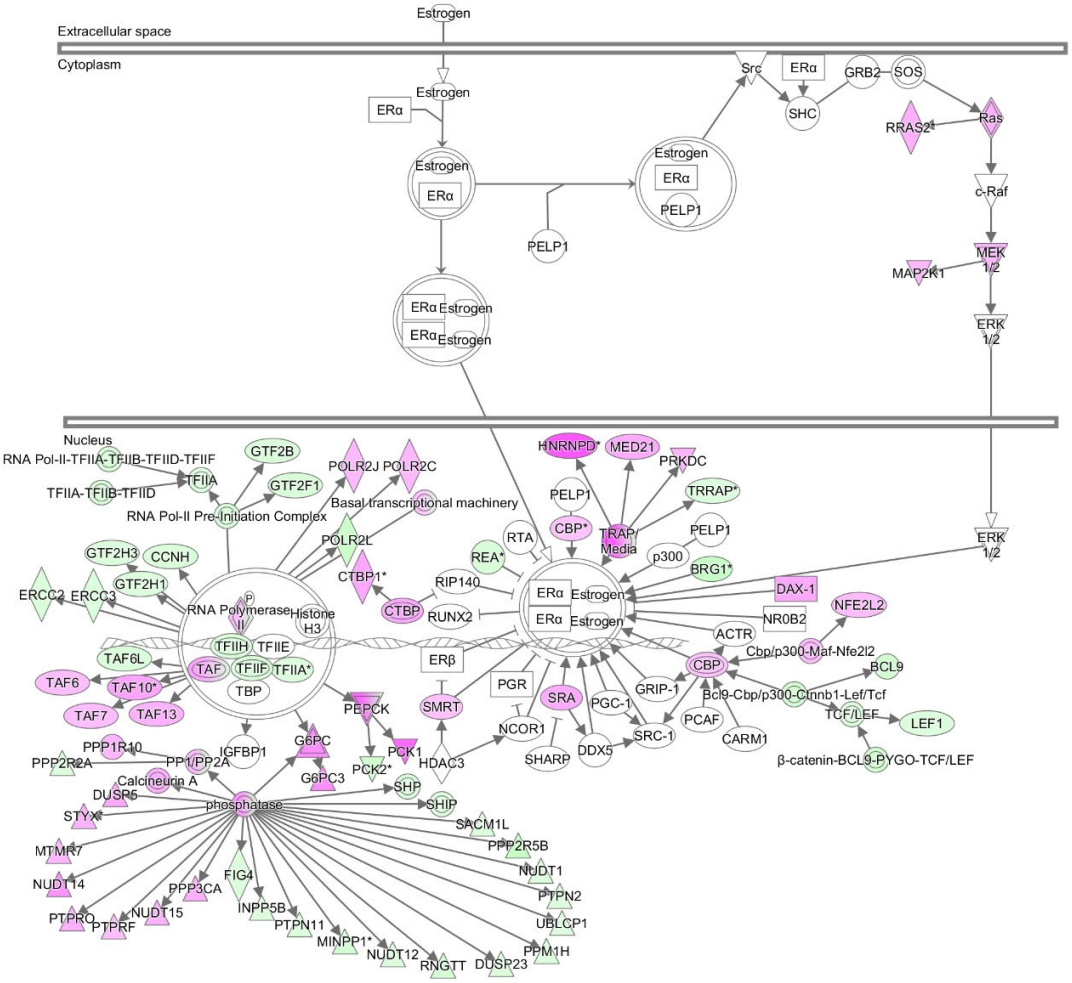

Fig. S2. Inactivation of estrogen receptor signaling under winter-like conditions. Genes in magenta and green are summer-induced and summer-repressed genes, respectively.

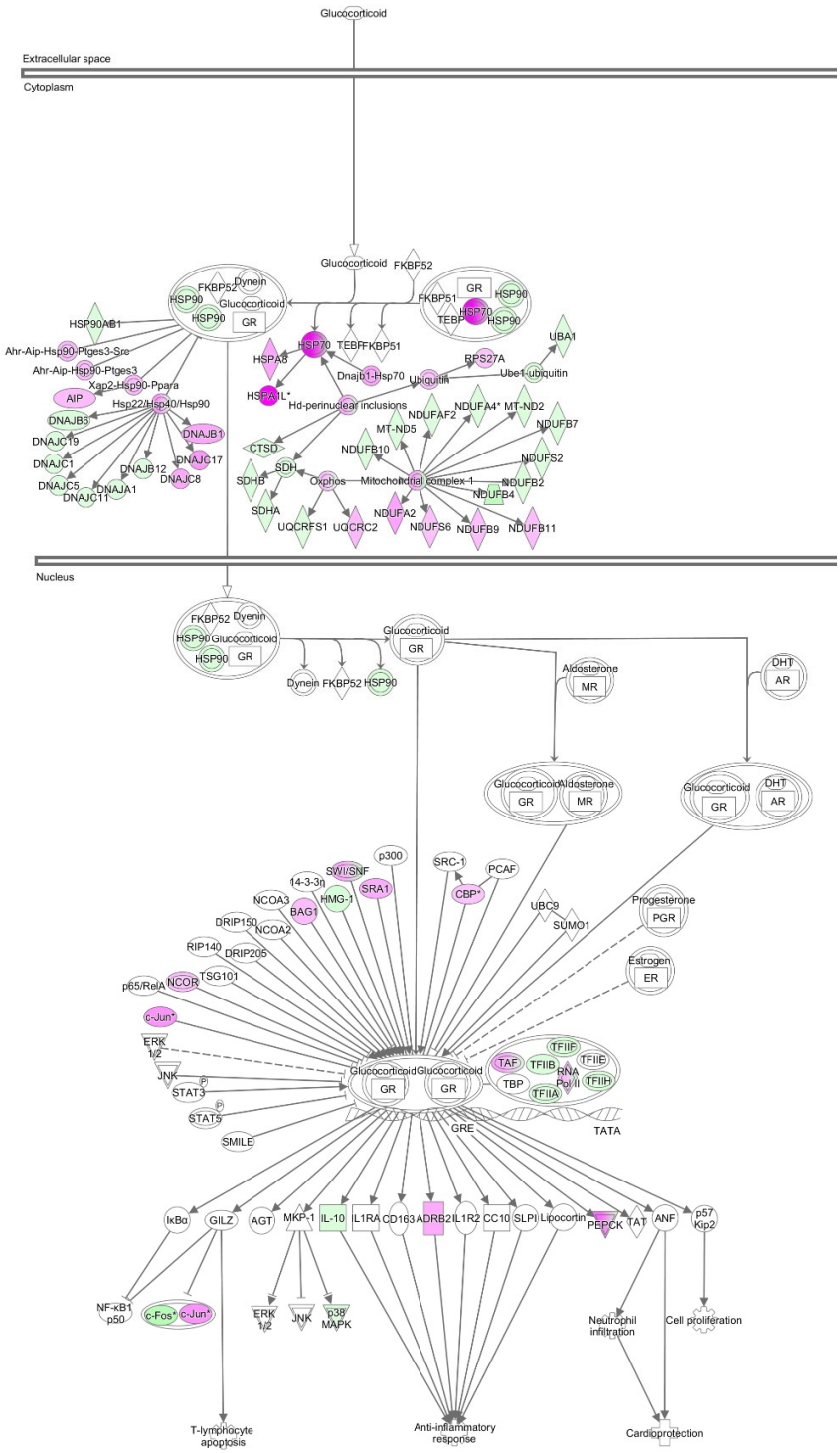

Fig. S3. Inactivation of glucocorticoid receptor signaling under winter-like conditions. Genes in magenta and green are summer-induced and summer-repressed genes, respectively.

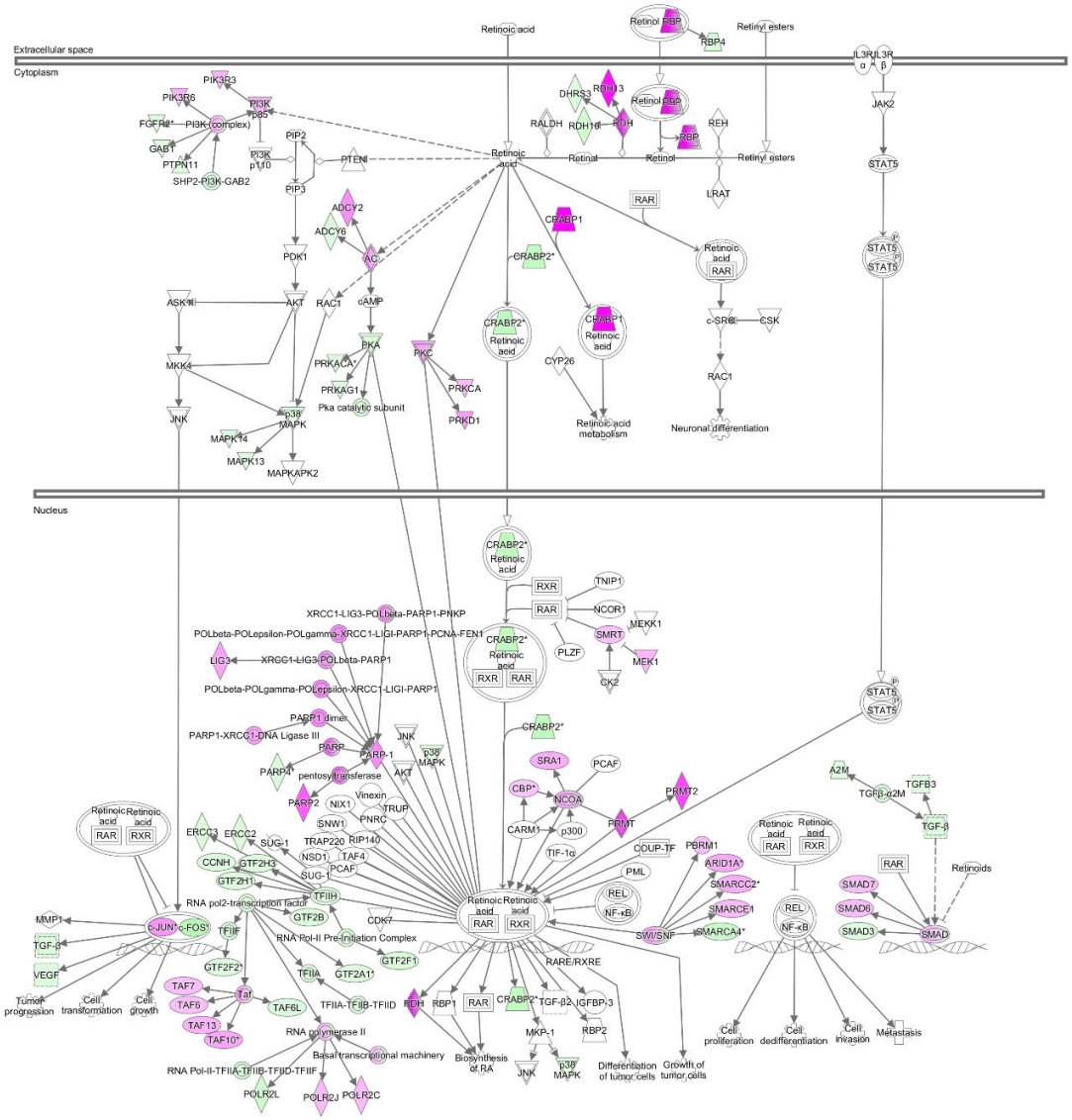

Fig. S4. Inactivation of retinoic acid receptor (RAR) signaling under winter-like conditions. Genes in magenta and green are summer-induced and summer-repressed genes, respectively.

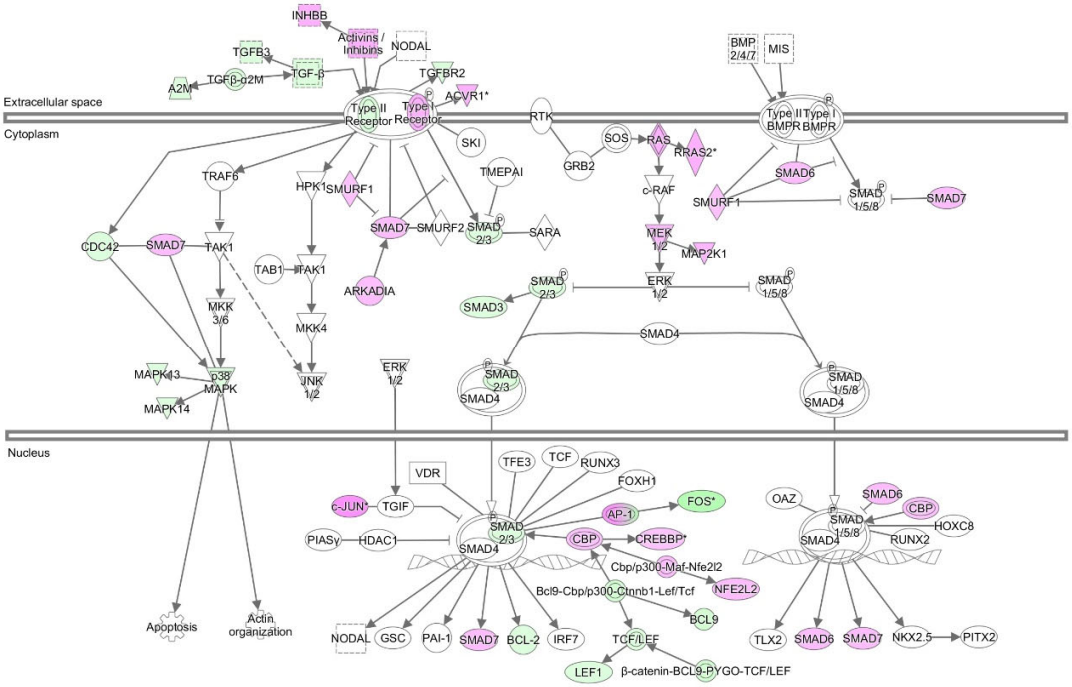

Fig. S5. Inactivation of activin signaling under winter-like conditions. Genes in magenta and green are summer-induced and summer-repressed genes, respectively.

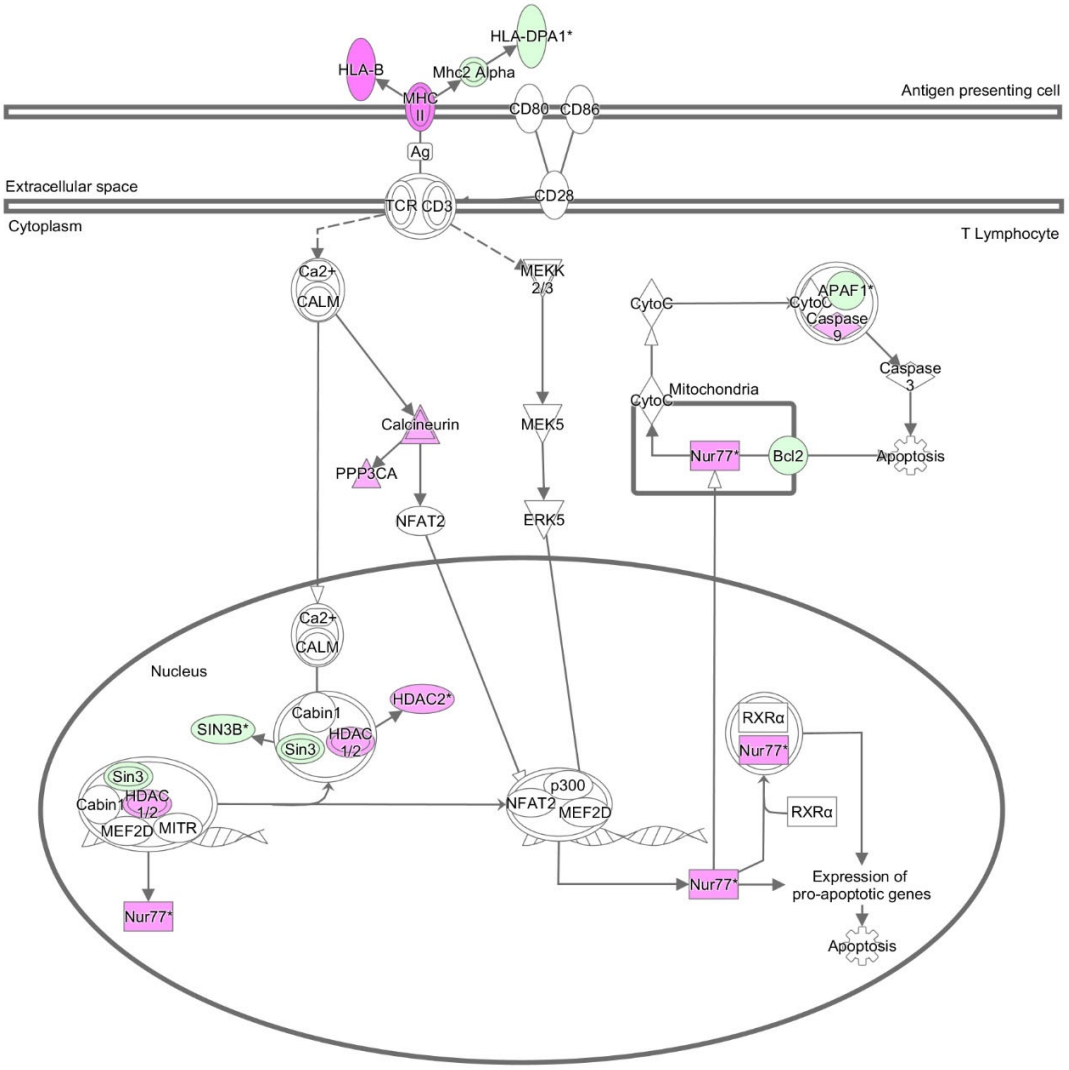

Fig. S6. Inactivation of Nur77 signaling under winter-like conditions. Genes in magenta and green are summer-induced and summer-repressed genes, respectively.

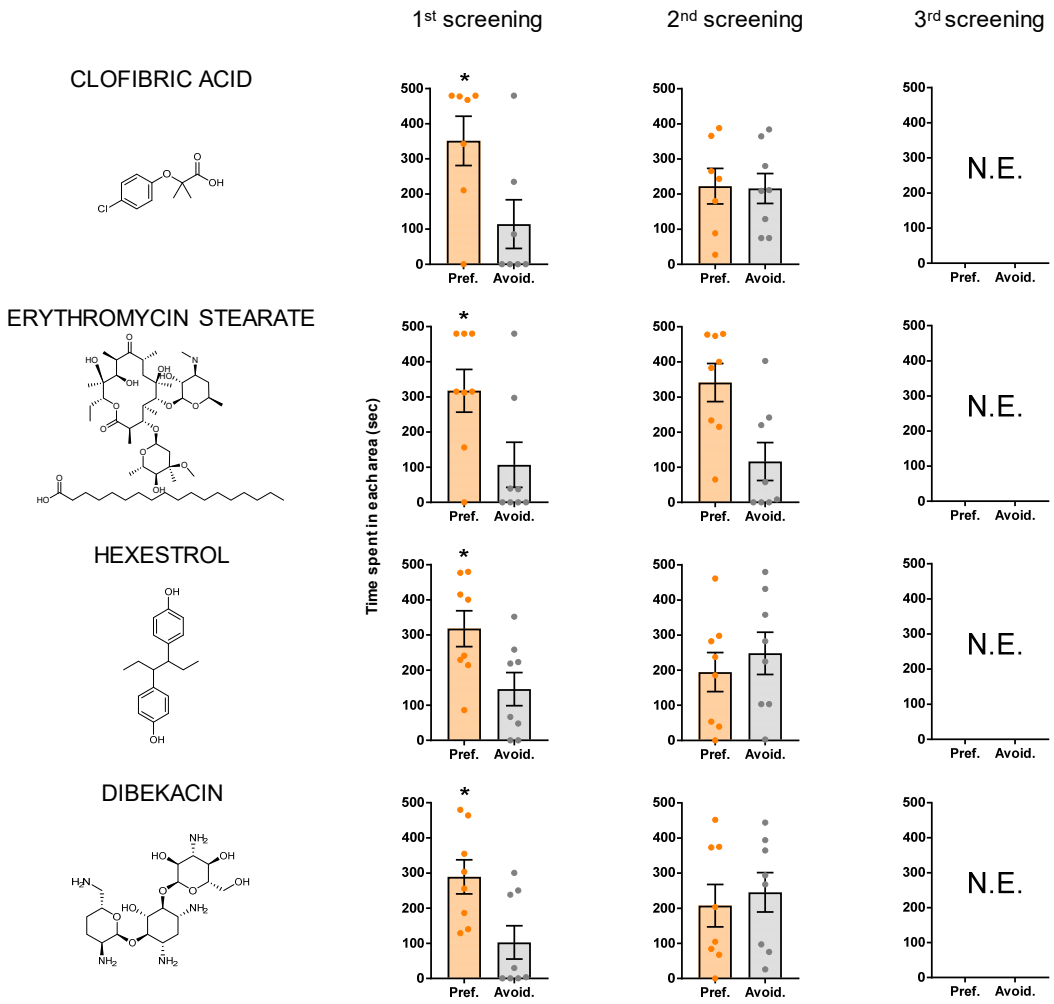

Fig. S7. Effect of all potential hit compounds on the three-chamber sociability test. From the first screen of 112 existing drugs, 21 potential hit compounds were identified, which were then reexamined by different experimenters (2nd and 3rd screen). Celastrol was the only compound that had consistent effects and passed all three screens; therefore, all other potential hits were excluded from further analysis. Chemical names and structures for each potential hit compound are shown on the left side of the results for the three-chamber sociability test. Results are presented as the mean ± SEM. Data were analyzed by Welch's *t*-test (**P* < 0.05, ***P* < 0.01, 1st and 2nd screen: n = 8; 3rd screen: n = 15). N.E.: not examined.

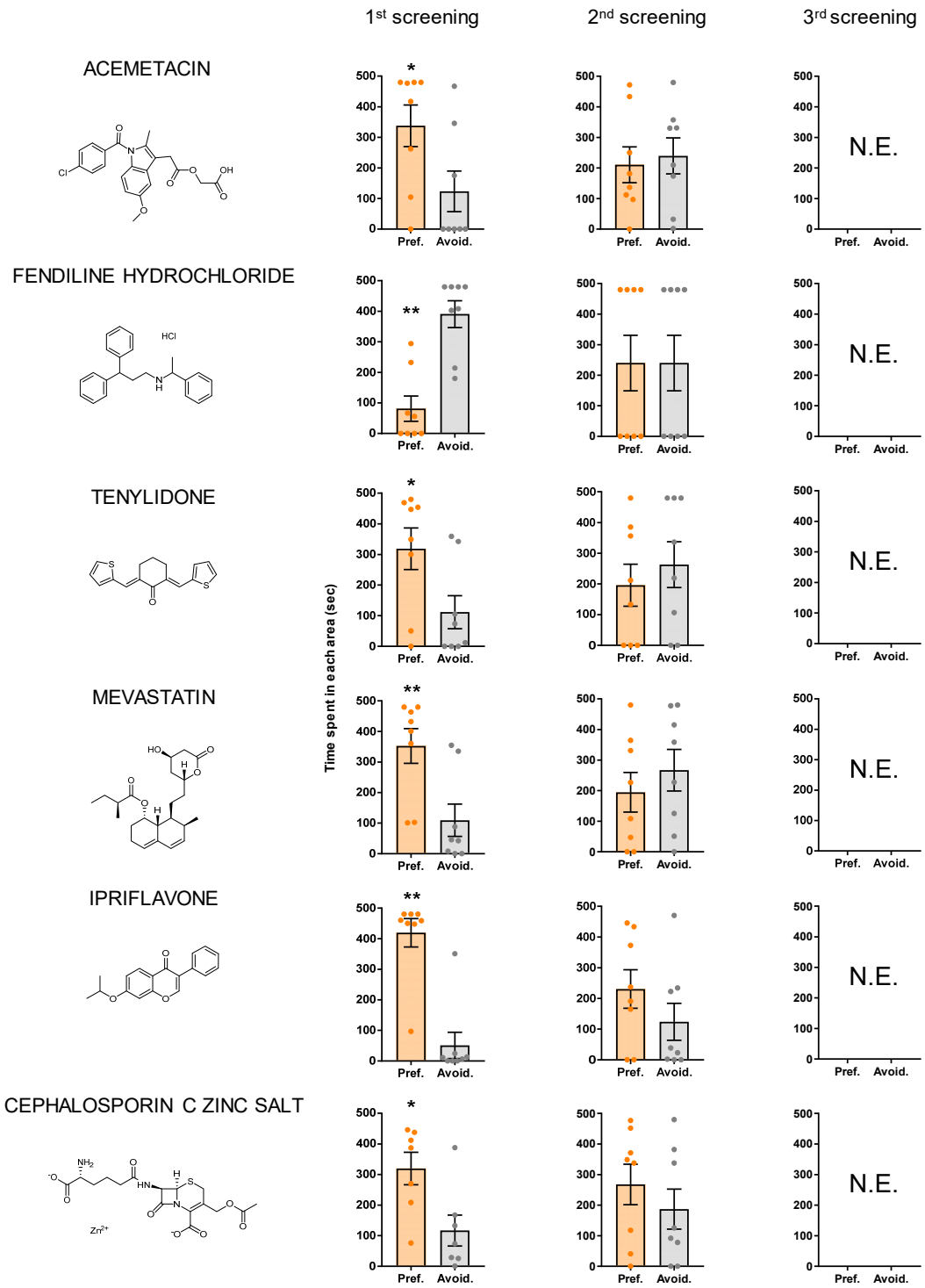

Fig. S7. (continued)

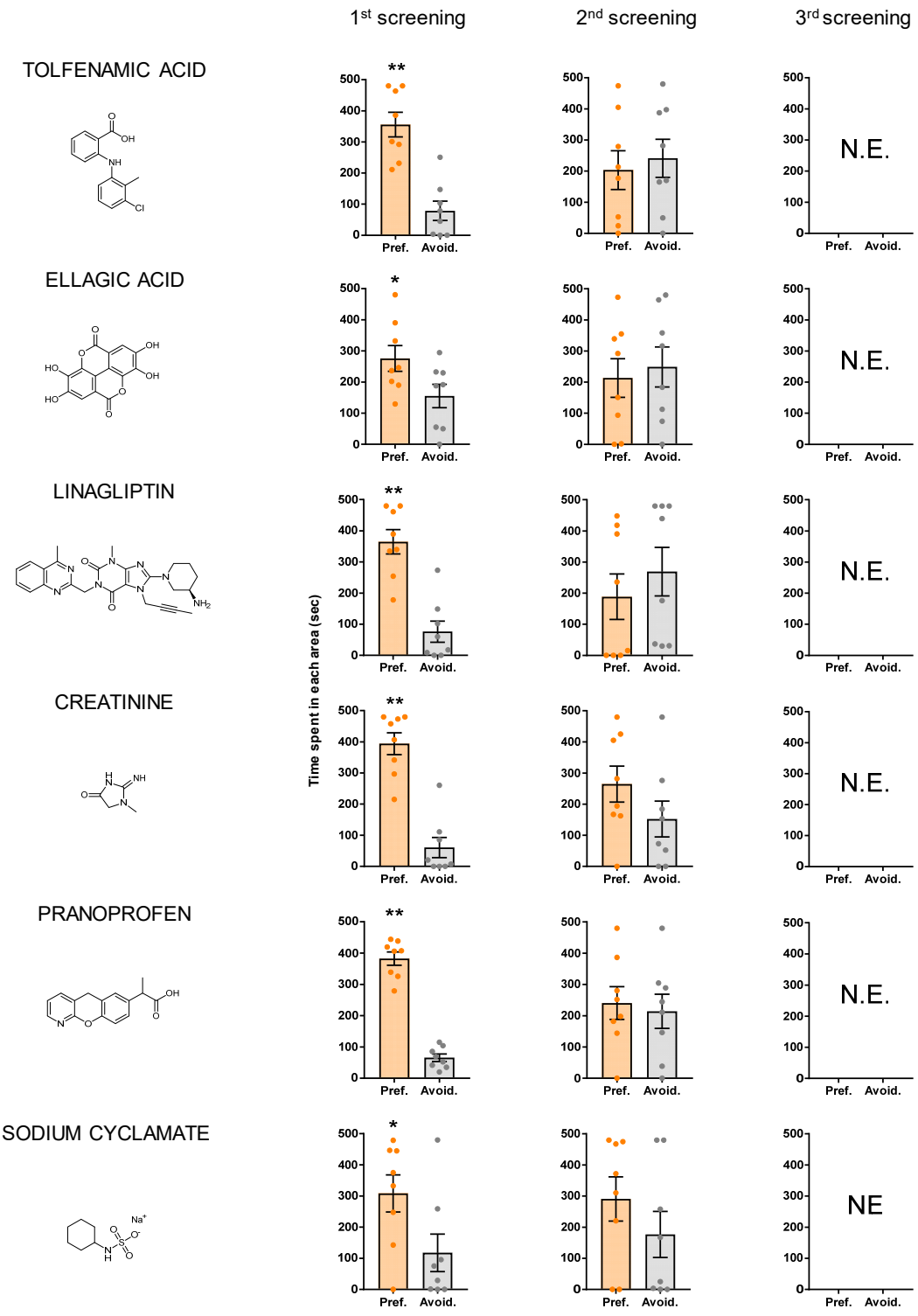

Fig. S7. (continued)

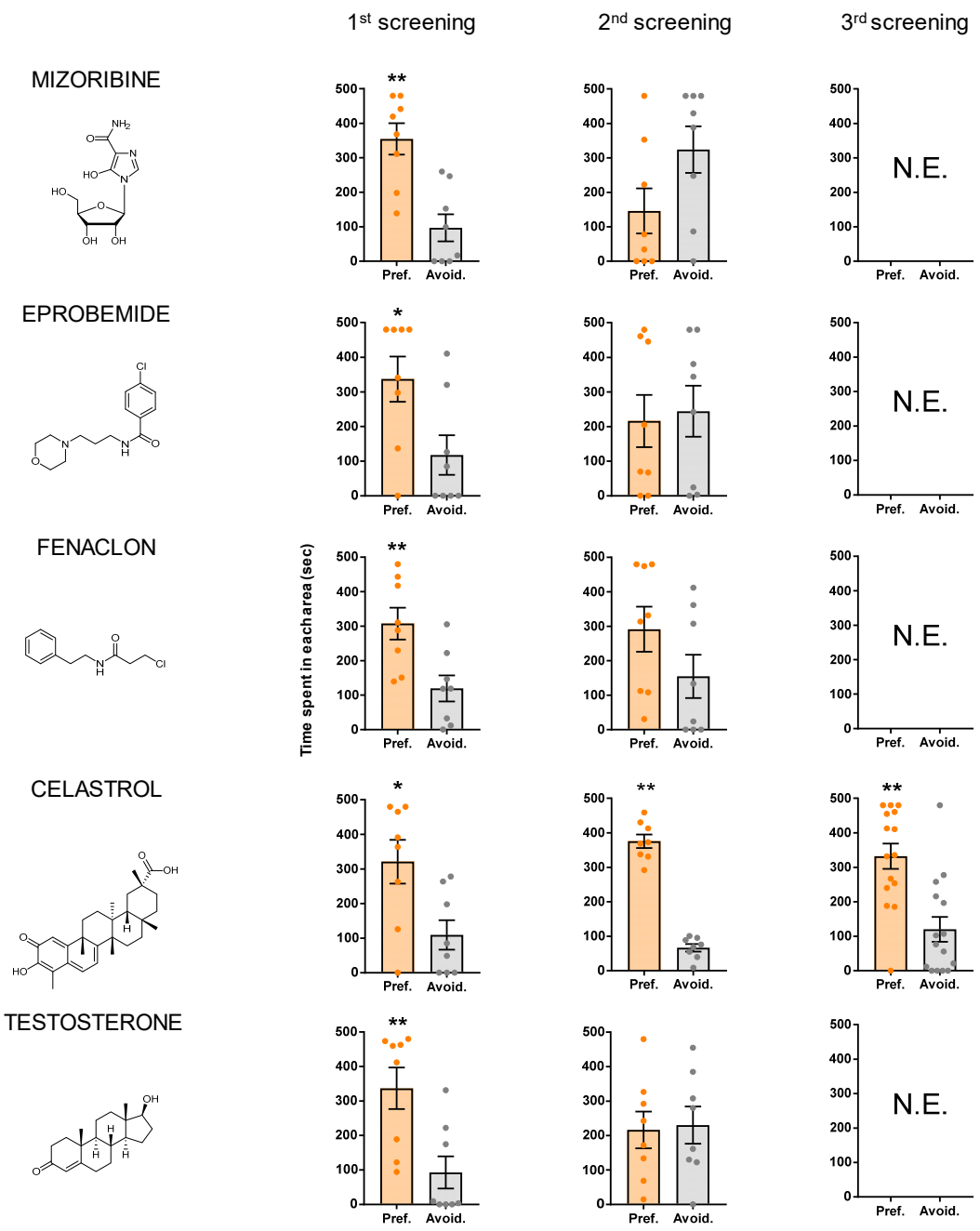

Fig. S7. (continued)

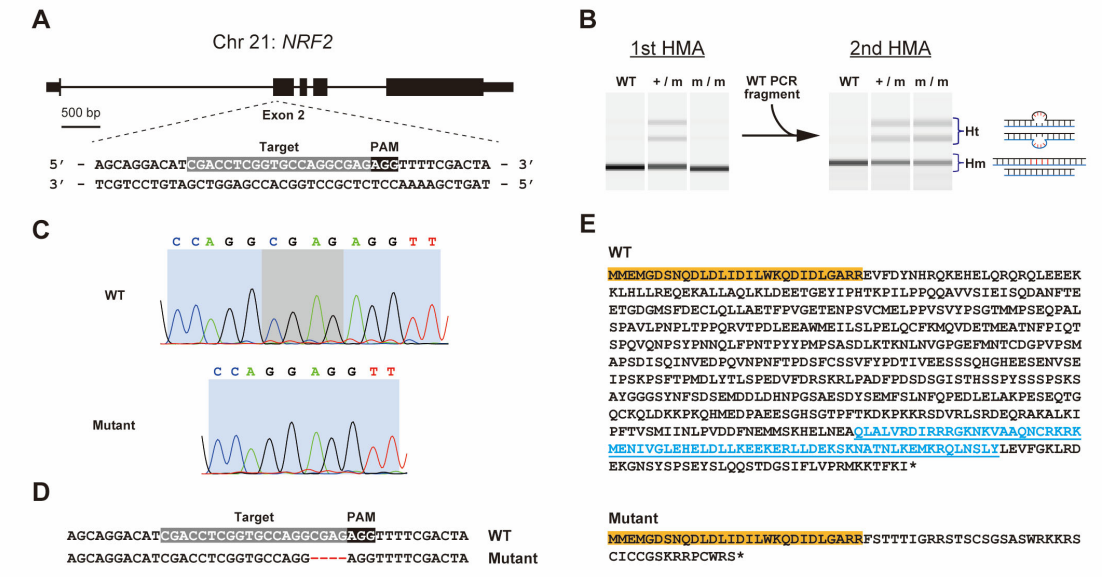

Fig. S8. Generation of CRISPR/Cas9 *NRF2* mutant medaka. (*A*) The *NRF2* locus targeted by the CRISPR/Cas9 system. The black solid boxes represent *NRF2* exons. The gray and black boxes with white characters highlight the targeted sequence and the NGG protospacer adjacent motif (PAM) sequence, respectively. (*B*) PCR fragments obtained from genomic DNA of wild-type, heterozygous and homozygous mutant fish analyzed using a heteroduplex mobility assay (HMA) with a microchip electrophoresis system. The first assay (1st HMA) identified heterozygote fish, which showed heteroduplex bands. To clearly define wild-type and homozygous mutant fish, samples were reannealed with PCR fragments amplified from wild-type genomic DNA, and a second assay (2nd HMA) was performed[58]. This assay identified a homozygous mutant, which showed heteroduplex bands. Hm, homoduplex; Ht, heteroduplex. (*C*) Chromatogram of direct DNA sequencing of the *NRF2* gene. The gray background shows the region deleted in mutant fish. (*D*) *NRF2* mutant medaka had a 4-bp deletion in exon 2 of the *NRF2* gene. (*E*) Predicted amino acid sequence of the NRF2 protein in wild-type and *NRF2* mutant medaka. The 4-bp deletion in exon 2 resulted in a frame shift mutation and premature stop codon upstream of the DNA binding and dimerization domains. Orange boxes highlight the region in wild-type and mutant NRF2 unaffected by the mutation and is thus identical. Thereafter, the mutant sequence diverges from the wild-type and terminates prematurely. Blue characters show the DNA binding and dimerization domains, which are completely missing from the mutant protein.

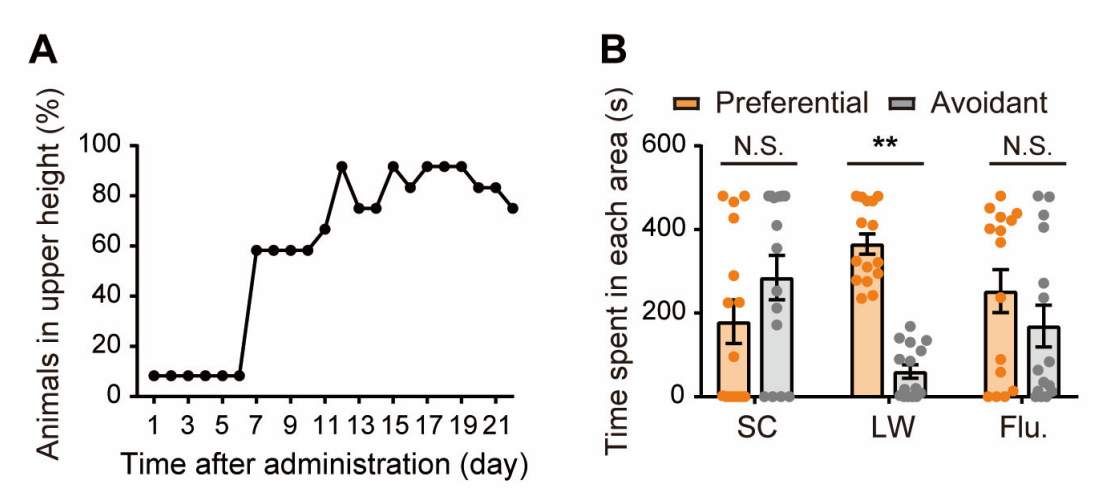

Fig. S9. Fluoxetine partially mimics the effect of summer conditions on behavior in medaka. (*A*) Daily administration of fluoxetine (0.8 μM) induced medaka to swim at the top of the tank, reflecting reduced anxiety-like behavior in winter-like conditions (n = 12). (*B*) Two-week fluoxetine treatment did not mimic the effect of summer conditions on behavior of medaka in the three-chamber sociability test (two-way ANOVA and Sidak's multiple comparison test. ***P* < 0.01, N.S. is not significant, mean ± SEM, n = 15).

Supplementary Tables

Table S1. Measured metabolites in the metabolomics analysis

Table S2. Differentially-regulated metabolites between SC and LW conditions

Table S3. Differentially-expressed transcripts between SC and LW conditions

Table S4. Rhythmicity of circadian clock genes expression

Table S5. Drugs used for the chemical screen

Table S6. Differentially-expressed transcripts between DMSO- and celastrol-treated fish

Table S7. Primer sequences used in the qPCR

References

1. A. Rodriguez, D. B. Ehlenberger, D. L. Dickstein, P. R. Hof, S. L. Wearne, Automated three-dimensional detection and shape classification of dendritic spines from fluorescence microscopy images. *PLoS One* **3**, e1997 (2008).
2. T. Hiraki, *et al.*, Female-specific target sites for both oestrogen and androgen in the teleost brain. *Proc. R. Soc. B Biol. Sci.* **279**, 5014–5023 (2012).